# OSCULATING CONE WAVERIDERS: A FLEXIBLE METHODOLOGY FOR HYPERSONIC VEHICLE DESIGN

MARK J. LEWIS*

*Department of Aerospace Engineering, University of Maryland*
*College Park, Maryland 20742, USA*

The hypersonic waverider concept includes the class of configurations that are designed so that their bow shockwaves are attached to the leading edge. Waveriders were first introduced with an inverse-design approach, in which a generating body is used to construct a virtual flowfield, from which an efficient aerodynamic shape is derived for a certain set of desired properties. Choosing that initial generating body had proven a source of great uncertainty, until Sobieczky introduced his concept of the "osculating cone" solution. Because the method begins with a desired shock, not a chosen generator, it lends itself to greater flexibility, a more inclusive optimization space, and the ability to more closely tailor waverider-like properties to existing generic hypersonic forms.

## 1. Introduction

### *1.1. High Lift Low Drag Shapes*

Classic reentry vehicles, including planetary probes, manned capsules, and the Space Shuttle, have been designed to mitigate high heating rates with blunt leading edges that also create significant drag, thereby enabling deceleration from orbital velocities. Interest in accelerating hypersonic vehicles – for aircraft, weapons, maneuvering reentry, and access-to-space, has fueled an extensive body of research at the opposite end of the high-speed aerodynamic design spectrum, namely low-drag lifting bodies.

An efficient craft that will be accelerating and maneuvering must be designed to fly through the atmosphere with minimum drag. Such vehicles will have relatively slender shapes with thin leading edges at the front of the aircraft, with smallest possible wave and viscous drag under the constraints of materials-imposed heating limits.

Incorporating these sharp configurations in a practical configuration means adopting a whole new design paradigm: using the shock wave to our best advantage, instead of fighting it. One very promising design is the so-called waverider airfoil, named because it rides on top of its own shock wave for highly efficient flight. Waverider geometries are of special interest for hypersonic applications because they offer the promise of higher lift-over drag, *L/D,* than generic hypersonic bodies.[1-6] A waverider may be thought of as any supersonic geometry with its bow shock attached to the leading edge.

Nonweiler first proposed Waveriders in 1957, as a possible solution for gradual reentry.[7] Though never effectively used for that application, they were incorporated into high-speed aircraft designs (e.g. the XB-70 prototype bomber) and more recently, fight testbeds (e.g. X-43A, X-51)

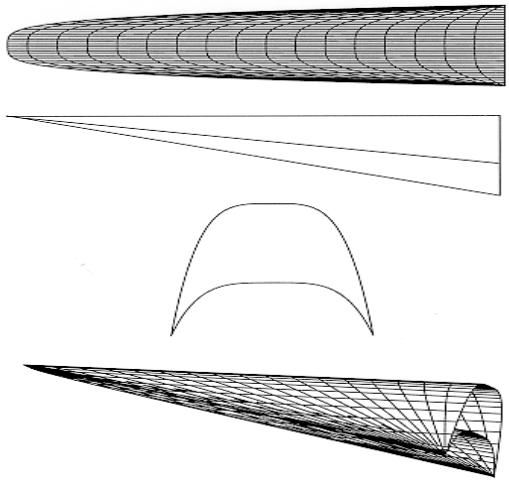

**Figure 1. Typical waverider shape derived for on-design shock attachment, high volume, and maximum *L/D*.**

Experiments on Nonweiler's early shapes confirmed that they had relatively little wave drag, but they tended to have significant viscous drag because of large surface area-to-volume ratios, as well as poor packaging because of the low volumetric efficiencies. Subsequent work, including especially the contributions of Rasmussen, expanded the waverider design envelope to include viscous considerations, greater volumetric efficiencies, etc.[8] Computational fluid techniques further expanded the design space. However, it wasn't until Sobieczky introduced the unique concept of the "osculating cone" solutions in the early 1990's that waveriders became a more flexible construct, and "waveriding" could be added as a property to existing generic shapes. In a sense, Sobieczky single-handedly changed the waverider concept from a noun to an adjective.[9]

* Currently: Chief Scientist of the U. S. Air Force
1075 Air Force Pentagon, Washington DC 20330

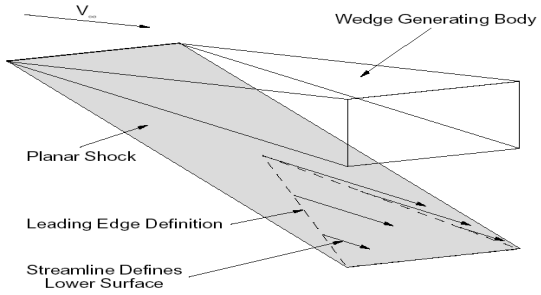


**Figure 2. Inverse waverider design. Flowfield shown will yield a Nonweiler "caret" geometry.**

### *1.2. Waverider Design Methodologies*

Waveriders are supersonic shapes in which the bow shockwave is directly attached to the leading edge. This means that all of the flow that passes through the shockwave on the lower lifting part of the waverider is contained below the waverider. This has the benefit of producing a generally high value of available *L/D* with high lift coefficient, and reducing cross flow and non-uniformities on the compression surface. It also provides for efficient flow capture into an inlet at a specific design condition. Waveriders were first defined by Nonweiler using simple 2-D flowfields.[7] Nonweiler's approach was an inverse solution, in which a flowfield is first chosen, then a waverider is selected from within that field.

In fact, waveriders can be designed either directly[10] or inversely, the defining criterion being that the flow-wise leading edge oblique angle must be smaller than the attachment angle for a supersonic shockwave. Nonweiler's solution introduced the method of waverider generation by starting with a known flow associated with a chosen shape in a supersonic freestream, as shown in Figure 2. Within that flow, and its known shockwave, a stream surface parallel to the direction of flow under the wedge is selected to represent the lower surface of the waverider. The intersection of that lower surface and the original shockwave defines the leading edge with an attached shockwave. This process works because the supersonic flowfield is mathematically hyperbolic, so that the carved-out section that forms the waverider surface, representing perhaps a small portion of the original flowfield, still retains the properties of that flowfield even though the generating body has been ignored once the waverider is defined.

A lingering question in the design of a hypersonic waverider has been the choice of best generating shape. Nonweiler's original work used simple wedge flows to form the shockwave because of their ease of calculation. Other generating bodies can be used as the starting point of the waverider flowfield design process. Conically-derived waveriders have been used extensively because they tend towards higher volumetric efficiency than the wedge-derived forms, yet still lead to relatively simple analytical solution. Even with the choice of a cone generating body, there is still a choice to be made of the cone angle for a given Mach number.

Rasmussen explored the design envelope of conical waveriders extensively, examining cone and perturbed cone solutions to seek the best generating flow from which to carve an optimal waverider. Rasmussen also introduced a process to optimize a waverider shape for its overall drag including skin friction, not just wave drag, leading to an extensive body of literature in optimized solutions and the reintroduction of waverider shapes as practical airframe configurations.

With the introduction of modern computational techniques, the choice of waverider generating bodies was greatly expanded. Nearly any supersonic flowfield could be used as a starting point for such a process. Axisymmetric powerlaw shapes were chosen as a logical step, with the reasoning that powerlaw shapes have less wave drag than cones, so powerlaw-derived waveriders should have less drag than cone-derived forms. That reasoning turned out to be false, as the streamsurfaces that determine the pressure distribution, and hence, drag, on an axisymmetric body were not necessarily incorporated into the final waverider shape.

Complex shapes were also enabled with computational solutions. For instance, combinations of cones and wedges have also been explored for creating the generating flowfield.[11] Wedge-derived waveriders have tended to have better *L/D* and more uniform flows than cones, but conically-derived waveriders tend to be more volumetrically efficient. The idea behind the hybrid was to seek the best of both forms. For a given flight Mach number, both the wedge and cone-shaped forms have only one degree of freedom: the oblique surface angle. In combination, the wedge-cone generator offered a second degree of freedom, the width of the wedge section relative to the cone radius. For any given cone/wedge oblique angle, a cone-wedge hybrid could be formed that tends to be more "cone-like" or more "wedge-like." The method proved very useful in fitting waverider shapes to existing generic forms.

Interestingly, a cone-wedge hybrid form was selected for the NASA Ames SHARP L1 proposed flight experiment in 2000, shown in Figure 3, but it is not a waverider.[12] The chosen form was designed for high lift in reentry, as a flight testbed for high-temperature ceramic leading edge materials. The designers chose a cone-wedge generator itself rather than a waverider that would have been carved from some portion of the flowfield of a cone-wedge hybrid. The vehicle was intended as the third in a series for flights, but though the first two simple flight experiments were successful, this lifting body was never actually flown.

In fact, building on this idea of the cone-wedge generator, nearly any shape that has associated with it a shockwave and supersonic downstream flow can be used as the initial generating body for a waverider. In turn, each generating flowfield contains an infinite number of stream surfaces, which can be selected to form the final waverider, so there is great flexibility in the process, and it is ripe for the

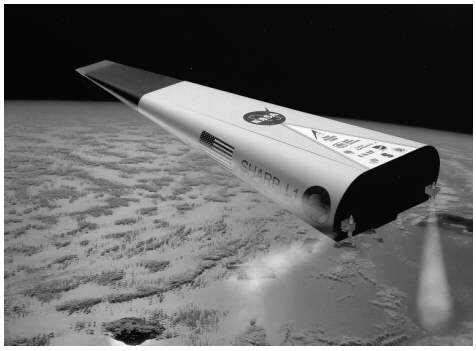

**Figure 3. Proposed NASA-Ames SHARP L1 reentry experiment, using a hybrid cone-wedge geometry. From Reference 12.**

application of optimization. However, there is still no direct means of identifying the best flowfield from which to carve the waverider, and thus no means of determining a truly optimal configuration using inverse techniques. Father, inverse techniques were limited to relatively simple flowfields, two-dimensional or axisymmetric, because in the absence of a clear means of optimizing, simple solutions remained as valid as any others.

Another solution to this was a forward waverider generating technique, explored by Starkey and Lewis.[10] In this case, a simple mathematical model was constructed to describe a waverider with relatively few geometric parameters. This work showed that a wide envelope of optimized hypersonic shapes can be described well with simple powerlaw functions to describe the planform area, projected at some effective oblique angle, and the base area, and indirectly the shock layer and degree of uniformity in the undersurface flow. Then, by varying the powerlaw coefficients and amplitudes, a very large variety of geometries could be explored analytically.

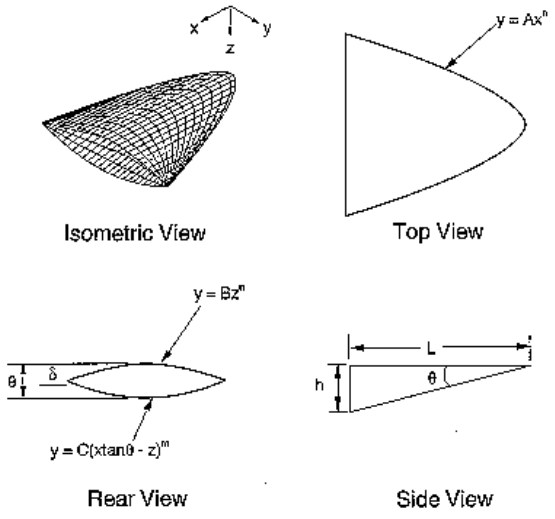


**Figure 4. Basic geometry description for parametric hypersonic waverider forward design.**

A geometry derived in this manner is shown in Figure 4, which demonstrates a lifting body design with convex upper and lower surfaces. As shown, the full geometry definition requires only six variables:

- length, $l$
- leading edge angle, $\delta$
- ventral angle, $\theta$
- amplitude constant, $A$
- planform coefficient, $n$
- base curvature coefficient, $m$

where the upper surface is assumed oriented to freestream.

This simple description proved extremely flexible and robust, and could include nearly any class of contiguous-surface vehicles without complex curvature. For instance, setting $n$=$m$=1 so that the planform is triangular produces Nonweiler's original so-called "caret" shaped waverider form. Similarly, setting $n$=0.5 resulted in shapes that closely resembled waveriders derived from conical flows.

For a concave compression surface, as is characteristic of inward turning and come waverider forms, $\theta<\delta$; for convex compression surfaces, more characteristic of generic forms, $\theta>\delta$. Not all combinations of variables are permitted. It is important that realistic geometric constraints not be violated; For instance, it is necessary to require that the vehicle have positive thickness at all planform locations. Other constraints could be placed on the geometry generator, including whether the lower surface is convex or concave, and even if the planform or volume fit within a prescribed box size. That means that this geometry description meshed well with optimization procedures, so that parametrics could be performed easily and rapidly, then confirmed with an optimization process.

Local surface angle can be calculated directly from the prescribed surfaces:

$$\phi_{\text{local}} = \tan^{-1}\left\{\frac{\left(\frac{y}{A}\right)^{\frac{1}{m}}(\tan\delta-\tan\theta)l^{\frac{1-n}{m}}+l\tan\theta-\left(\frac{y}{A}\right)^{\frac{1}{n}}\tan\delta}{l-\left(\frac{y}{A}\right)^{\frac{1}{n}}}\right\} \quad (1)$$

With this known, inviscid lift and drag are derived from pressure, calculated with either tangent wedge or tangent cone solutions, integrated over the surface. This technique provided great flexibility in exploring a given design space, and provided the streamwise leading edge angle is within the shock attachment limit for a given Mach number, produced valid waverider forms. However, the details of the resulting flowfield were somewhat unknown, and could only be derived computationally. This might prove unacceptable for engine-airframe integrated systems, in which knowledge of inlet flowfield properties would be key to the appropriate integration of a functional propulsion system.

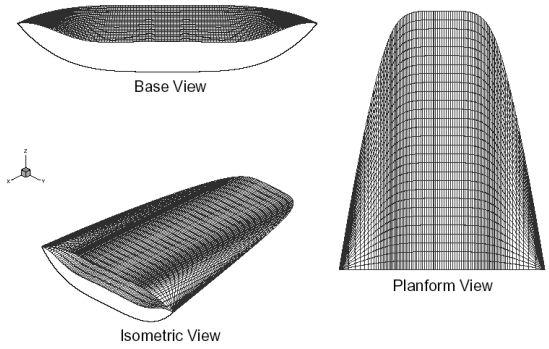


**Figure 5. Typical osculating cone waverider, in this case derived for Mach 10 with planer ventral flow and conical leading edge flow.**

### *1.3. Locally-Axisymmetric Flow*

Sobieczky developed a waverider generation technique that eliminates the need to choose a generating body and permits direct specification of the desired shock wave instead. It also offers many of the benefits of the forward techniques described above, while providing design information about the chosen flowfield. This is the so-called osculating (Latin for "kissing") cones waverider method. [13]

This technique is a shock-based solution that defines the flowfield directly from a specified shockwave, and allows the direct selection of inlet flowfield while providing good volumetrics and packaging. In so doing, it eliminates the need to select an initial generating body, with the associated uncertainty of choosing the "best" generator, and also allows for more direct fitting of waverider aerodynamics to basic generic forms.

The osculating cone design approach is motivated by Sobieczky's realization that certain complex three-dimensional inviscid flowfields can be approximated by locally two-dimensional solutions. For instance, a supersonic flow with streamlines that have varying azimuthal curvature can be approximated by a series of local conical flows, each of which is computed assuming constant radius of curvature corresponding to the actual local values.

The osculating cone method yields extremely flexible forms that combine the benefits of conical flows and planar flows as needed. Figure 5 presents a typical osculating cone result. The method is not exact, but rather approximates a three-dimensional flowfield as a series of two-dimensional planes. Several studies have already been performed to validate computationally and experimentally the osculating cone waveriders design. Takashima performed numerical simulations on osculating cone waverider shapes in order to integrate those as the forebody of a hypersonic vehicle[19]. The computational results at on-design conditions agreed with the general map of the analytical predicted flowfield, though shock resolution was inadequate to assess the match to desired accuracy.

Miller and Argrow tested two aluminum models of Mach 4 and Mach 6 osculating cone geometries[15] in the Mach 4 Unitary Plan Wind Tunnel and the Mach 6 blow down Tunnel of the NASA Langley Research Center, respectively. At on-design conditions the experimental results confirmed the predicted location of the shock wave. The measured surface pressure distributions generally agreed with the analytical predictions. That study also confirmed that the osculating cone waveriders provided the high promised hypersonic *L/D* values.[16] The particular shapes chosen in that study had small crossflow pressure gradients, and so the effects of neglecting those gradients should not have been significant.

In the 1990's, McDonnell-Douglas, now Boeing Phantom works, developed a concept for a hypersonic global cruise aircraft known by its generic name as the "Dual-Fuel Cruiser." This was vehicle was envisioned to fly a mission starting with hydrogen fuel up to half the Earth's circumference, then return to base with aerial refueling of hydrocarbon fuels. The basic design was a conically-derived waverider with truncated leading edges. A parallel effort was undertaken to produce osculating cone shapes that would match the basic mold lines of the baseline, but with improved lift-over-drag and more uniform inlet flow conditions. A series of 68 separate osculating cone solutions were derived, optimized for various combinations of lift and volumetrics.[17]

Ultimately, the baseline conical shape was chosen over any of the osculating cone shapes because the osculating cone solutions had wider planforms to provide perfectly uniform ventral inlet flows; this resulted in higher predicted transonic drag. The pure conical shape had non-uniform inlet flow properties, but there was no penalty for this. Aerodynamic performance was similar because the baseline and osculating cone solutions were waveriders, though the osculating cone solutions did exceed the baseline in all cases. Regardless, the osculating cone solution proved its utility in being able to add "waveriderness" to existing hypersonic shapes, and in being able to produce such a high number of geometries for optimization in a very short period of time. The final configuration of the Dual Fuel vehicle formed the basis of NASA's X-43 Hyper-X flight test vehicle, that reached Mach 7 and Mach 10 in 2004.[18]

More recently, osculating cone solutions have been used in various designs for proposed hypersonic vehicles. Lockheed-Martin had developed a configuration for hypersonic cruise that shows remarkable similarity to shapes associated with Sobieczky's osculating cone solutions, as shown in Figure 6.[19] Note that in this figure, the design has used the ventral pod-like structures that are characteristic of osculating cone solutions for locating engines, although flowfield uniformity issues in those areas make such integration questionable.

## 2. Osculating Solution Steps

### *2.1 Locally Two-Dimensional Assumption*

In the method of osculating cones, the generating flow is defined by a design Mach number, a bow shock angle, and a shock wave shape at the exit plane of the waverider. As a result, the method does not require a generating body to be defined. The flow field behind the non-axisymmetric shock is determined by assuming "locally conical" flow in the normal planes along the shock curve.

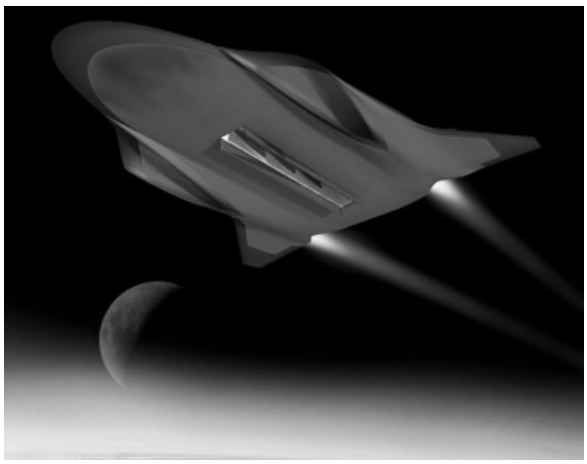

**Figure 6. Hypersonic vehicle concept, using osculating cone-type geometry. From Reference 19.**

The ``locally conical" flow is defined by an osculating slice of flowfield. The osculating cone method does in fact produce a "virtual" flowfield generator associated with the specified shockwave, but the designer need not identify this directly. Not all shock solutions are physically permitted; some would correspond to non-physical generators or intersecting flowfield slices. Wedge-derived waveriders and cone-derived waveriders may be thought of as limiting cases of the osculating cone waveriders method; wedge-derived forms correspond to on osculating region with an infinite radius of curvature, and cone-derived ones correspond to one with a constant radius of curvature.

The vertex of the conical flowfield in each plane is determined by the local radius of curvature and the shock angle. The shock curve is chosen so that the change in the radius of curvature is continuous along the curve, and a series of planes is used along the shock curve in the exit plane to fully define the flow field behind the bow shock.

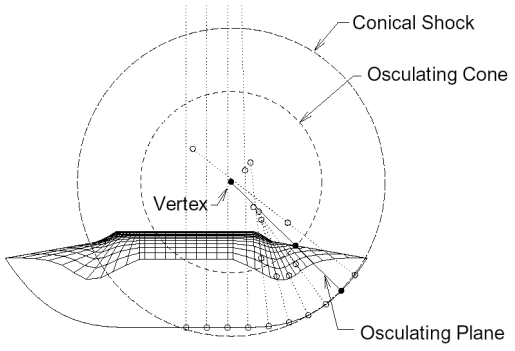


**Figure 7. Construction of a complex waverider form using osculating cones. Note the characteristic ventral lobes that form as the shock transitions from highly curved to nearly 2-D. Adapted from Reference 9.**

A constant radius of curvature exactly reproduces a conical flowfield; and infinite radius results in wedge-like flow. Thus, the osculating cone methodology can span the gamut from caret shapes to conically derived, with many combinations in between. This process is shown in Figure 7. Note that the osculating cone solution captures many of the desirable features of the hybrid cone-wedge method outlined above, but without the uncertainty of having to define the relative dimension of wedge width to cone radius, in addition to the cone (and thus wedge) angle. Also unlike the hybrid method, the extent of uniform flow can be exactly defined to match desired flowfield properties, such as for an inlet. This last property has been used to advantage in numerous design studies, including that of O'Brien and Lewis.[6] Figure 8 presents an integrated vehicle form that was designed at Mach 12 for perfectly uniform inlet conditions.

### *2.2 Taylor-Maccoll Solutions*

Because the osculating cone solution builds a flowfield from axial slices of conical flow, the properties of the shocklayer in each slice are derived from the classic Taylor-Maccoll equations[20,21,22]:

$$\frac{d^2\bar{V}_r}{d\theta^2} = \frac{\bar{V}_r\bar{V}_\theta^{\,2} - \frac{\gamma-1}{2}\left(1-\bar{V}_r^{\,2}-\bar{V}_\theta^{\,2}\right)\left(2\bar{V}_r - \bar{V}_\theta\cot\theta\right)}{\left[\frac{\gamma-1}{2}\left(1-\bar{V}_r^{\,2}-\bar{V}_\theta^{\,2}\right)\right]-\bar{V}_\theta^{\,2}} \qquad (2)$$

$$\bar{V} = \frac{V}{V_{\max}} = \frac{V}{\sqrt{2C_pT_{o_\infty}}} \qquad V_\theta = \frac{dV_r}{d\theta} \qquad (3,4)$$

This ordinary differential equation is readily integrated, for instance with a fourth-order Runge-Kutta method.

In the basic osculating cone solution, the flowfield is defined from a prescribed shockwave and intersecting leading edge; in various formulations, powerlaw functions are used for simplicity to define these curves. Local tangent, or "osculating" cones are traced along the prescribed shockwave shape at each discrete point. The radius of the osculating cone

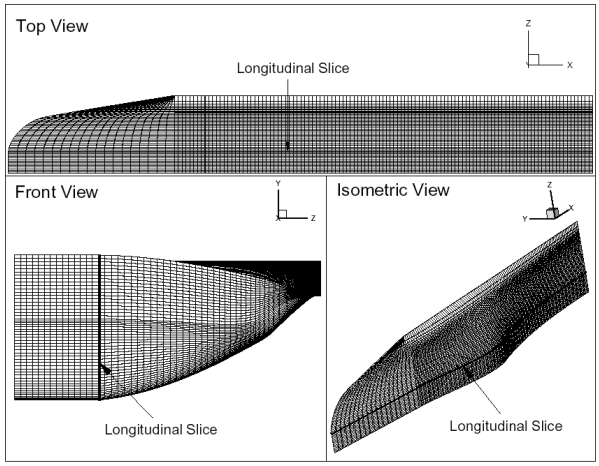


**Figure 8. Osculating cone-derived waverider for a Mach 12 configuration. From Reference 6.**

is just the local radius of curvature of a virtual generating surface. The intersection of the prescribed leading edge curve and the local osculating shock has to be determined. The longitudinal position of the leading edge is determined by projecting the previous leading edge point in the streamwise direction: the vehicle leading edge occurs at the intersection of the shockwave surface generated by the local osculating cone and the proscribed leading edge curve. The upper surface of the vehicle is then obtained by projecting each leading edge point downstream to the base plane. The entire shockwave is determined by marching upstream along each local osculating cone surface, from the base plane to the leading. With the known shock geometry, the shock layer properties can be determined directly from Taylor-Maccoll.

In Sobieczky's original formulation, the resulting predicted flowfield does not account for pressure gradients between the osculating cone slices. Since the flow is built from adjacent regions of locally-conical flow, but each with a unique local azimuthal shock curvature, there should actually be some crosswise flow that is not accounted for in the basic method. This means that, strictly speaking, the generated osculating cone flowfield is not an exact match to the original conically-constructed flow. That in turn raised some questions as to whether osculating cone solutions were actually waverider forms, and also whether they would have the delivered performance that is predicted by their constructed flows.

As it turns out, in nearly all practical cases these neglected pressure gradients are minimal. In fact, they can be corrected, but the resulting waverider shapes and associated flow properties closely resemble the uncorrected osculating cone shapes derived by Sobieczky. Figure 9 presents this induced pressure on one Mach 6 waverider.

In general, osculating cone shapes have demonstrated flow properties that are very close to the original predicted flows, despite the fact that they are not exact solutions. For instance, Figure 8 presents pressure contours of the flow on the undersurface of the Mach 12 waverider in Figure 6.

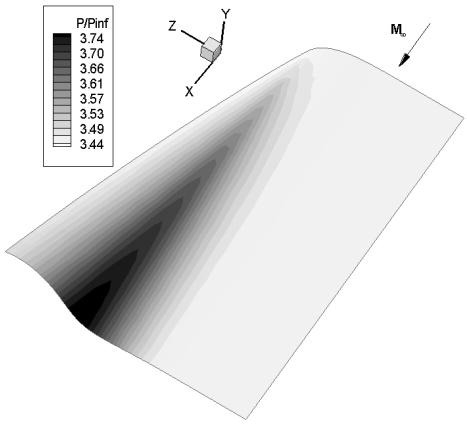


**Figure 9. Pressure distribution on the lower surface of an osculating-cone waverider. From Reference 23.**

The top of this figure shows the predicted analytical result, whereas the bottom shows the computed response. Note the very close match between predicted and computed contours.

Despite this generally good agreement, and the positive results of experimental efforts such as those of Miller and Argrow.[15] It has recently been of interest to characterize possible errors introduced into the osculating cone process, and, if possible, mitigate them as part of the design methodology.

## 3. Modified Osculating Cone Solution

### *3.1. Unaccounted Pressure Gradients*

Recall that Nonweiler's original waverider concept used body-derived flowfields, those that begin with an assumed flowfield associated with a chosen generator.[7] Because the generator must be chosen first, this exact approach can have restrictions on the flowfield properties; for instance, waveriders that start with inviscid flow over a cone will always have inviscid conical flow in the final derived flowfield, no matter how complex the surface geometry. The same is not true of the osculating cone solutions.

In the recent efforts of Lewis and Chauffour[23] a simple predictor-corrector algorithm has been applied using Euler's flow equation to modify velocity, imposing a crosswise velocity component away from the gradient: $dV=-dp/rV$. Some recent results are shown in Figure 11. which presents the magnitude of corrected velocity on an osculating cone waverider lower surface.

Sobieczky's osculating cone method solves this problem by starting directly from a desired shockwave shape, not a generating body.[13] Slices of flow from the Taylor-Maccoll cone solutions are then assembled from the shockwave, derived as a function of local shock radius. This makes for a more flexible solution, one which can be more easily fit around desired inlet geometries, volumetric considerations, etc. [14]

### *3.2. Pressure Gradient Corrections*

Since osculating cone solutions are built from slices of conical flows with varying radii of curvature they are not exact, as they neglect the cross-flow pressure gradients that would result between adjacent conical flow slices. The present work introduces a simple methodology to account for

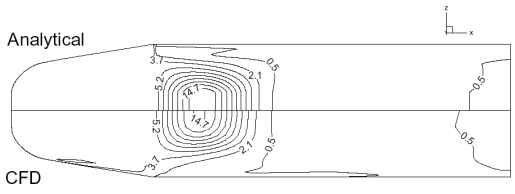


**Figure 10. Pressure contours on the undersurface of a Mach 12 osculating cone-derived waverider vehicle. From Reference 6.**

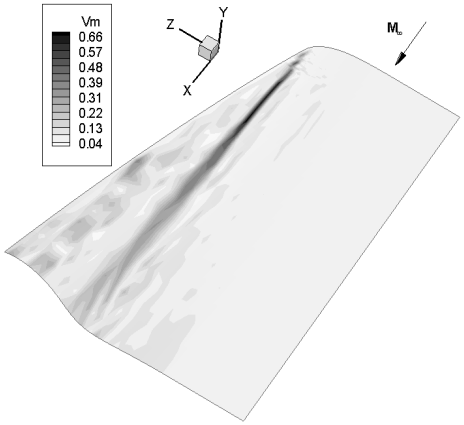


**Figure 11: Velocity correction on the lower surface of an osculating cone design. From Reference 23.**

the azimuthal pressure gradients. Because the generated flowfield is entirely inviscid, Euler's equation, $dV^2 = -2\,dp/\rho$, is applied to determine the local pressure gradients between each osculating cone slice. At each streamwise plane, a velocity correction is applied between adjacent points in the azimuthal direction:

$$\begin{aligned}\left(\Delta V_i^2\right)_{corr} &= -\frac{2}{\rho_i}\Delta P_i \\ &= -\frac{2}{\rho_i}\left(\frac{P_{i+1} - P_{i-1}}{2}\right) \\ V_i &= V_i + \sqrt{\left(\Delta V_i^2\right)_{corr}}\end{aligned} \qquad (5)$$

Typical results of this correction, for shapes with large gradients at Mach 3 and Mach 6, are presented in Figure 12 and Figure 13, respectively. These views show half of the osculating cone waverider base with both an original form and a pressure-corrected solution. Note that in neither case is the modified geometry significantly different than the original design. This suggests that previous osculating cone solutions are actually quite accurate, and azimuthal pressure gradients should be small.

For the Mach 3 waveriders, some geometric differences between the corrected lower surface and the uncorrected lower surface can be observed in Figure 12. Not surprisingly, the modifications introduced by the correction method are most significant primarily in the region where the gradients of shock wave curvature are the highest, which is where the highest spanwise pressure gradients are located. For the Mach 6 waverider in Figure 13, differences between uncorrected and corrected forms are less significant. At Mach 10, the inclusion of azimuthal pressure gradient introduces virtually no significant changes.

### *3.3. Calculated Flowfield Changes with Modification*

Computational solutions were obtained to evaluate the impact of the geometry modifications of the pressure corrections on the waverider flowfield. The inviscid flowfield predicted by the analytical solution of the osculating cone

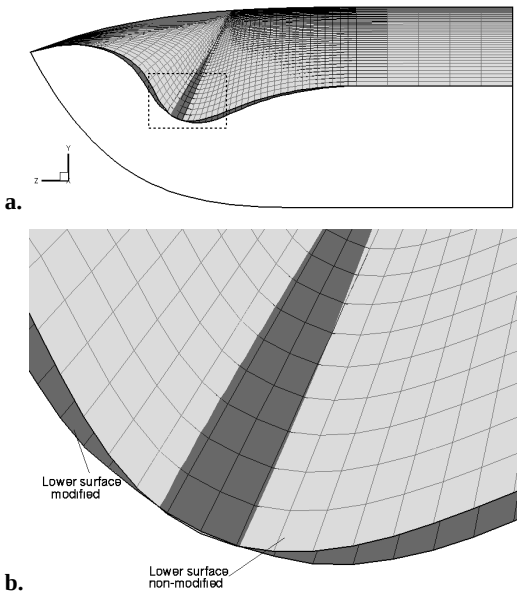


**Figure 12. Half of the base plane of an osculating cone waverider, derived for flight at Mach 3, showing both the original and "corrected" solutions in part a. The region of highest gradient, indicated by outline in part a, is expanded in part b. From Reference 23.**

(1) generating flowfield was compared to the results from an inviscid computational simulation obtained with CFD-FASTRAN from CFD research Corporation, a fully implicit finite volume code using local time. At each time step, flux vectors were evaluated using Roe's upwind flux difference splitting, with an Osher-Chakravarthy flux limiter in order to achieve third-order spatial accuracy. The solutions were allowed to converge until the $L_2$ norm of the density residual dropped at least by three orders of magnitude. The change in lift and drag coefficients were also less than $10^{-3}$ over 100 iterations. Finite volume grids were constructed using a Cartesian grid generator, CFD-GEOM.

Waverider configurations present the double challenge of a sharp leading edge, with a strong shock wave attached to it; the grid was locally refined in order to capture the solutions details at the leading edge and to sharply resolve the gradients associated with the shock wave. Computational grids were shock-fitted in order to reduce freestream points, with 100x100x70 points around the waverider half-body.

A comparison of the normalized base pressure contours at Mach 6 is presented for both an uncorrected and corrected waverider in Figure 14 and Figure 15, respectively. Design shock angle is $17^o$, with a design altitude of 28 km, corresponding to a velocity of 1800 m/s and *L/D* approximately 4. The shock was selected to provide nearly planar flow down the ventral axis, and conical flow near the leading edge. In both cases, the predicted shock wave location agrees very well with the CFD result. Also in both cases, the pressure contours exhibit some smearing in the azimuthal direction though the uncorrected waverider shows more distortion and pressure contours deviate more from

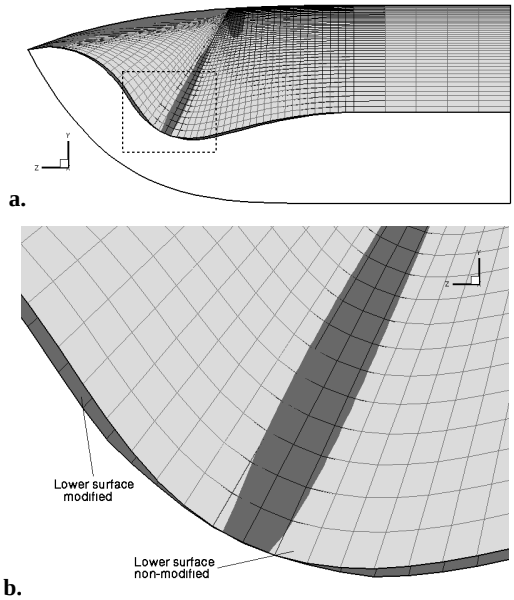


**Figure 13. Half of the base plane of an osculating cone waverider, derived for flight at Mach 6, showing both the original and "corrected" solutions in part a. The region of highest gradient, indicated by outline in part a, is expanded in part b. From Reference 23.**

purely conical form. Note also that the uncorrected waverider shape has a smaller region of ventral flow uniformity, though the differences are subtle. Overall, the differences between corrected and uncorrected osculating cone solutions are indeed small for this chosen example, and though the azimuthal correction adds little computational complexity, a form derived without it would still offer good agreement between predicted and derived performance. As the Mach number increases the flow tends to become unidirectional in the streamwise direction; as a result the influence of azimuthal pressure gradients becomes even less significant.

Interestingly, the overall aerodynamic performance of the corrected and uncorrected designs are nearly identical; the lift coefficient calculated for the corrected waverider, $C_L$=0.0496, is 0.106% higher than the analytical prediction for that shape; that of the uncorrected waverider, $C_L$=0.0485,

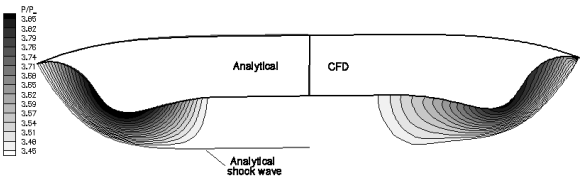


**Figure 14. Computational solution of an unmodified osculating cone waverider, showing a comparison of pressure contours in the base plane. From Reference 23.**

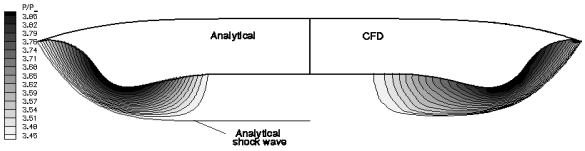


**Figure 15. Computational solution of a pressure-corrected osculating cone waverider, showing a comparison of pressure contours in the base plane. From Reference 23.**

is 0.196% lower. However, the overall *L/D* of the uncorrected shape (both predicted and calculated) is actually higher than that of the corrected one by about 0.5%, dropping from 3.92 to 3.90 with the azimuthal correction. These small differences suggest some interesting trends but are of minimal practical significance. Indeed, with the addition of viscous effects, such differences are little more than an analytical curiosity. Note that at high altitude, rarefied effects can further detract from osculating cone waverider behavior; in fact, that can be true of any waverider form.[24]

## 4. Conclusions

Sobieczky's method of osculating cones introduced a new design technique for optimizing high-lift hypersonic shapes, and solved an ongoing problem of selecting the best flowfield by avoiding the problem all together. Whereas previous work had concentrated on identifying the best generating body from which to form a waverider, Sobieczky simply avoided the question by seeking an entirely different approach, one that begins with the shockwave.

Osculating cone solutions has thus far demonstrated the highest lift-over-drag of any known waveriders, with the ability to tailor flowfields that fit generic, non-waveriding airframes, or that provide desired engine inlet properties. By developing a method that seamlessly combines conical and wedge-based flowfields, Sobieczky's technique makes available the best of both known solution types, with great flexibility for exploiting the benefits of both two-dimensional and axisymmetric flow patterns.

A lingering issue had been that osculating cone solutions were not exact because they neglected transverse pressure gradients, and thus some question remained about whether the derived analytical solutions could be applied to realistic configurations. In fact, computational and experimental solutions had shown excellent agreement with prediction, but that was for specific geometries that may not have had extreme pressure gradients. Corrections for leading-edge bluntness, viscous effects, etc. should also introduce far greater errors into the final design than neglecting transverse pressure gradients.

To settle this question, a modified osculating cone waverider design technique has been introduced. When applied, the derived geometry could be modified to provide a better match between predicted analytical flowfields and actual computed flowfields, especially in the location of pressure gradients. However, it was observed in chosen test cases that only small modifications were seem in the streamlines. The differences between the corrected and non-

corrected configurations are most significant in the regions of highest gradient of the shock wave curvature. Note that the pressure correction technique could be run iteratively, until some convergence is reached. It is not known if that would be a stable process, but it was clear that, for the chosen waverider examples, such iteration was unnecessary.

Research since the early 1990's has found Sobieczky's original waverider osculating cone concept to be a flexible, powerful tool for hypersonic vehicle design. The basic assumptions in Sobieczky's original waverider method have been well validated, and it has been shown that deviations from analytical solutions due to the azimuthal pressure gradients along the waverider geometry are negligible at sufficiently high Mach number (over Mach 4-5). This conclusion is of course dependent on the particulars of the individual waverider design. However, for nearly any practical osculating cone waverider geometry, the method has repeatedly been demonstrated to be an effective tool for vehicle integration and optimization.

**References**


1. M. K. L. O'Neil, M. J. Lewis, "Design Tradeoffs on Scramjet Engine Integrated Hypersonic Waverider Vehicles," *Journal of Aircraft*, Vol. 30, No. 6, 1993, pp. 943-952.

2. M. Lobbia, M., and K. Suzuki, "Numerical Investigation of Waverider-Derived Hypersonic Transport Configurations," AIAA Paper 2003-3804, Jun. 2003.

3. M. J. Lewis and A. D. McRonald, A. D., "Design of Hypersonic Waveriders for Aeroassisted Interplanetary Trajectories," *Journal of Spacecraft and Rockets*, Vol. 29, No. 5, 1992, pp. 653-660.

4. D. Strohmeyer, T. Eggers, and M. Haupt, "Waverider Aerodynamics and Preliminary Design for Two-Stage-to-Orbit Missions, Part 1," *Journal of Spacecraft and Rockets*, Vol. 35, No. 4, 1998, pp. 450-458.

5. W. Heinze, A. Bardenhagen, "Waverider Aerodynamics and Preliminary Design for Two-Stage-to-Orbit Missions, Part 2," *Journal of Spacecraft and Rockets*, Vol. 35, No. 4, 1998, pp. 459-466.

6. T. F. O'Brien, and M. J. Lewis, "Rocket Based Combined-Cycle Engine Integration on an Osculating Cone Waverider Vehicle," *Journal of Aircraft*, Vol. 38, No. 6, 2001, pp. 1117-1123.

7. T. R. F. Nonweiler, "Aerodynamic Problems of Manned Space Vehicles", *Journal of the Royal Aeronautical Society*, Vol. 63, pp. 521-528, 1959.

8. M. Rasmussen, *Hypersonic Flow*, Wiley and Sons, Hoboken, New Jersey, 1994.

9. H. Sobieczky, F. Dougherty, and K. D. Jones, "Hypersonic Waverider Design from Given Shock Waves," *Proceedings of the First International Hypersonic Waverider Symposium*, Univ. of Maryland, College Park, MD, Oct. 1990.

10. R. Starkey and M. J. Lewis, "Analytical Off-Design Lift-to-Drag Ratio for Hypersonic Waveriders," *Journal of Spacecraft and Rockets*, Vol. 37, Number 5, Sept.-Oct. 2000 pp. 684-691.

11. N. Takashima, and M. J. Lewis, "A Cone-Wedge Waverider Configuration for Engine-Airframe Integration," *Journal of Aircraft*, Vol. 32, No. 5, pp. 1142-144, September-October 1995.

12. D. Rasky, J. Salute, P. Kolodziej, "The NASA Sharp Flight Experiment," NTRS: 2004-11-03, ID 20020051881, NASA Ames Research Center, 1998.

13. K. B., Center, H. Sobieczky, and F. C. Dougherty, "Interactive Design of Hypersonic Waverider Geometries," AIAA Paper 91-1697, Jun. 1991.

14. N. Takashima, "Optimization of Waverider-Based Hypersonic Vehicle Designs," Ph.D. Dissertation, Dept. of Aerospace Engineering, Univ. of Maryland, College Park, May 1997.

15. R. W. Miller and B. M. Argrow, "Experimental Verification of the Osculating cone Method for Two Waverider Forebodies at Mach 4 and Mach 6," AIAA 98-0682, Jan. 1998.

16. K. D. Jones, H. Sobieczky, A. R. Seebass, and F. C. Dougherty, "Waverider Design for Generalized Shock Geometries," *Journal of Spacecraft and Rockets*, Vol. 32, No. 6, 1995, pp. 957-963.

17. N. Takashima, Takashima and M. J. Lewis, "Optimization of Waverider-Based Cruise Vehicles with Off-Design Considerations," *AIAA Journal of Aircraft*, Vol. 36, No. 1, Jan-Feb 1999, pp. 235-245.

18. L. A. Marshall, C. Bahm, G. P. Corpening and R. Sherrill, "Overview With Results and Lessons Learned of the X-43A Mach 10 Flight," AIAA 2005-3336, 13th International Space Planes and Hypersonics Systems and Technologies, Capua, Italy, May 16-20, 2005.

19. "Hypersonic Rocket-Plane Program Inches Along," *Defense Industry Daily*, 17 Mar 2005.

20. K. D. Jones, H. Sobieczky, A. R. Seebass, and F. C. Dougherty, "Waverider Design for Generalized Shock Geometries," *Journal of Spacecraft and Rockets*, Vol. 32, No. 6, 1995, pp. 957-963.

21. H. W. Leipman, and A. Roshko, *Elements of Gasdynamics*, Wiley, New-York, 1953, pp. 85-88.

22. G. I. Taylor and J. W. Maccoll, " The Air Pressure on a Cone Moving at High Speeds, I - II," *Proceedings of the Royal Society*, Ser. A, Vol. 139, No. 838, pp. 278 - 311, London, 1933.

23. M. J. Lewis, M. Chauffour, Shock-Based Waverider Design with Pressure Gradient Corrections and Computational Simulations Journal of Aircraft vol.42 no.5, 2005 pp. 1350-1352.

24. R. E. Graves and B. M. Argrow, "Aerodynamic Performance of an Osculating-Cones Waverider at High Altitudes," *AIAA-2001-2960*, AIAA Thermophysics Conference, 35th, Anaheim, CA, June 11-14, 2001